

Abstract

This study investigates the comparison of influences of CO₂ bubbling into the calcium hydroxide (Ca(OH)₂) slurry through a microbubble generator (MBG) and an ordinary CO₂ generator (OCG) on the preparation of calcite nanoparticles by a carbonation method. Each obtained precipitate was characterized using XRD, SEM and particle size analyses. During the carbonation process at each CO₂ flow rates, it was determined that the MBG generates tiny bubbles whereas an increase in CO₂ flow rates led to an increase bubble size when the OCG was used. The flow rate of CO₂ was not an important parameter with using the MBG as calcite nanoparticles were prepared (<125 nm) at each CO₂ flow rates. The necessary time for the complete reaction decreases with an increase in the CO₂ flow rates through the MBG in comparison to the OCG. To produce calcite nanoparticles with a high production recovery in shorter times, the MBG should be adopted to the carbonation reactor.

Keywords

CO₂ bubbles, microbubbles, calcite, nanoparticles

1 Introduction

Calcium carbonate (CaCO₃) is one of the most abundant materials and widely used as a filling material in various industries (paper, paint, plastic, rubber and so on) depending on its purity, opacity, whiteness degree, particle shape, rheology, specific surface area, particle size distribution, and water or oil absorption properties. However, the use of natural CaCO₃ particles is limited in the industrial applications as the controlling of those properties was difficult. Recrystallization processes (biomimetic method and carbonation method) have been conducted to prepare synthetic CaCO₃ particles with desired qualities [1].

The carbonation method is favorable in the industry because of the availability of raw material and low cost in comparison to the biomimetic method. CaCO₃ particles are prepared by absorbing CO₂ into a Ca(OH)₂ solution. However, the production recovery is not high yield due to low absorption of CO₂. The solubility of CO₂ is increased with the use of microbubble generator (MBG) that produces innumerable bubbles in micrometer-sizes [2].

Microbubbles are small spherical bubbles with 1 – 100 μm in diameter that can be uniformly suspended in a solution [3]. They have higher surface areas comparing to the conventional large bubbles [4]. They are generated by self-supporting generator, porous frit, sparger, double-tube gas injection nozzle, air-stone, ultrasonic probe, radial-shaped sparger, high shear circulation, multiple-orificer or membranes using different carbonation reactors [5-19].

The adaptation of those apparatus to the carbonation reactor leads to produce calcite nanoparticles with uniform morphology. The particle size of PCC was found to be 50 – 100 nm using the CO₂ bubbling orificer, whereas that of PCC in the absence of orificer was obtained in micron sizes [20]. It is obvious that MBG should be conducted to obtain calcite nanoparticles [5-7]. In addition, the particle size of PCC increased within increasing CO₂ flow rates. This paper reports the determination of influences of CO₂ flow rates using the MBG apparatus on the production of calcite nanoparticles by a carbonation method. The morphology, particle size and specific surface area of each precipitate were evaluated by SEM, XRD and particle size

¹ Department of Mining Engineering,
Faculty of Engineering and Architecture,
Çukurova University,
Balçalı, 01330, Sarıcam/Adana, Turkey

* Corresponding author, e-mail: maltiner@cu.edu.tr

analyses. The slurry pH was measured as an indicator for the complete reaction. Control experiments at the same conditions were performed using the OCG for the comparison.

2 Experimental

2.1 Preparation of calcite nanoparticles

In this study, 250 mL of 0.4 M $\text{Ca}(\text{OH})_2$ slurry prepared with an analytical grade $\text{Ca}(\text{OH})_2$ (Merck, purity $\geq 99\%$) and pure water was used for each experiment. Plexiglas reactor designed for producing calcite nanoparticles is shown in Fig. 1.

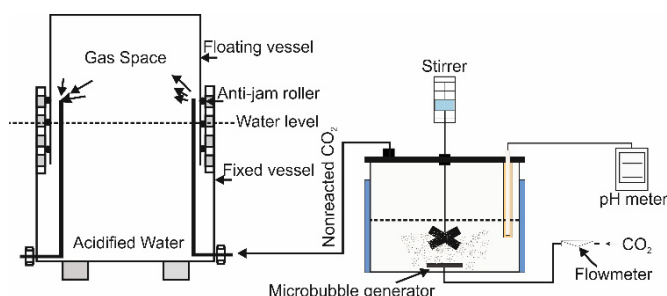


Fig. 1 Experimental set up for carbonation test

CO_2 (purity: 99.9%, supplied from Cargas, Turkey) with various flow rates (0.3, 1, 3, 5, 8 and 10 L/min) was bubbled into the $\text{Ca}(\text{OH})_2$ slurry through the MBG that was placed at the bottom of the reactor. The MBG has a porous structure and its length and diameter was 3 and 1 cm, respectively. With the use of this apparatus, tiny bubbles having same sizes are produced at each CO_2 flow rates. The dispersion of bubbles was better provided compared to the OCG. The duration time of each bubble generated through the MBG in the slurry was higher. The bubble size was not influenced by the CO_2 flow rates. However, the increase of CO_2 flow rates led to an increase the bubble size when the OCG was used.

A mechanical stirrer stirred the solution at 650 rpm during the carbonation. The reaction temperature was kept 293 K by a water bath. The carbonation time was variable depending on the CO_2 flow rates. The solution pH was continuously measured by pH meter (WTW 3110) during the carbonation reaction. When the solution pH was 7.30 ± 0.10 , the CO_2 flow rate was switched off and the reaction was complete. Non-reacted CO_2 was accumulated above the acidified water in a lab scale gasometer for the re-use. After conducting each carbonation, the suspension was filtered using filter paper (Whatman, No.1).

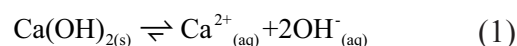
The precipitate was dried at 105 °C for 3 h in an oven in preparation for the characterization test. X-ray diffractometer (XRD, Rigaku) equipped with $\text{Cu K}\alpha$ radiation with the 2θ range of 15–85°, with a step size of 0.02 was performed. The diffraction data was identified using a PDXL software. The crystallographic properties of PCC were using a scanning electron microscope (SEM, Philips XL 30S FEG and Zeiss EVO LS-10). The average particle size of each precipitate was examined using a Malvern Master sizer (Hydro 2000 MU).

The reactor was cleaned by HCl (5%) solution to remove carbonate particles sticking on the reactor wall and the MBG or OCG, and then rinsed with water. Each experiment was repeated twice. Furthermore, control experiments were performed with an ordinary CO_2 bubbles generator (OCG) for the comparison.

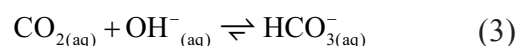
3 Results and Discussion

The pH value was an important indicator in the carbonation test. The decrease of pH indicates that OH^- ions are consumed and each Ca^{2+} ion is carbonated due to adding CO_2 gas. However, if the pH was ~ 9 , it is evident that the carbonation did not complete and the desired product is prepared because of the presence of OH^- ions in the slurry [21]. Precipitated calcium carbonate (PCC) production mechanism can be explained in the following equation (1) - (5) [22].

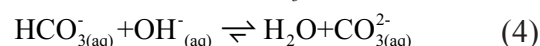
a) Dissolution of $\text{Ca}(\text{OH})_2$ to Ca^{2+} and OH^- ions



b) CO_2 absorption in water



c) The reaction between Ca^{2+} and CO_3^{2-} ions



Thereafter the reaction steps given below occurred, the PCC particles were formed in various morphological phases depending on the reaction conditions. It is thought that the dissolution of PCC particles is triggered with an decrease in the slurry pH. However, Han et al. [23] revealed that the PCC particles dispersed in the carbonate solution were not dissolved due to the high HCO_3^- concentration, when the slurry pH was about 7.50. Therefore, the carbonation reaction was terminated when the slurry pH decreased to the desired value.

The PCC particles are quite stable in the carbonate solution [23]. The behavior of solution pH during carbonation was explained by many researchers in the previous studies [25-27]. Wei et al. [25] explained that the behavior of slurry pH during the carbonation process divides into the two stages which are as follows: (1) constant rate of absorption stage and (2) falling rate stage.

In the first stage, more than 75% of the $\text{Ca}(\text{OH})_2$ is converted to PCC particles with the injection of CO_2 into the slurry and the formation of PCC particles is completed in the falling rate stage. However, Bang et al. [26] identified the hatched region area (HR) on the pH graph where steep changes in pH occurred with an injection of CO_2 . They claimed that Ca^{2+} ion was formed as PCC particles before the HR region. The slurry pH

did not change during the carbonation stage as the OH^- ion was supplied by the dissolution of $\text{Ca}(\text{OH})_2$ in the slurry until none remains [27]. The decreasing trends of the slurry pH during the carbonation were similar with those of previous studies. In this paper, the behavior of the slurry pH was evaluated based on the approach of Bang et al. [26]. The changes of pH in the slurry during the carbonation using the OCG and MBG are shown in Fig. 2 and Fig. 3, respectively.

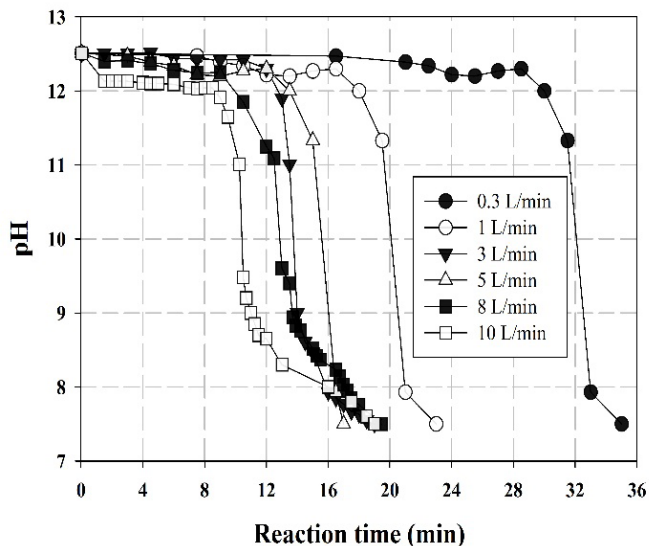


Fig. 2 Change in the slurry pH during carbonation using an OCG

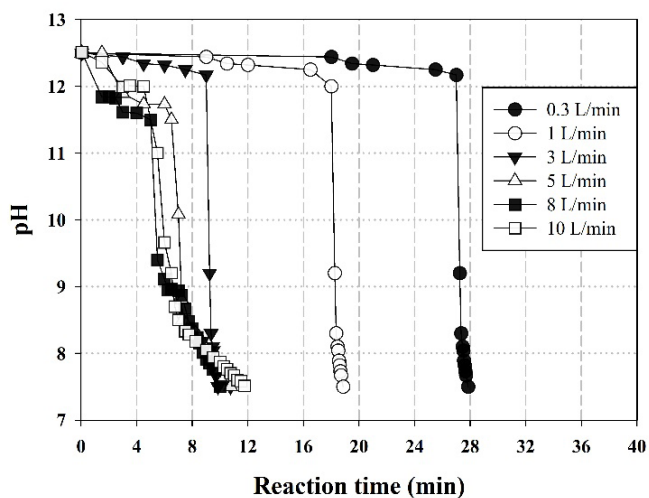


Fig. 3 Change in the slurry pH during carbonation using a MBG

The absorption ratio of CO_2 was lower than that of the dissolution rate of $\text{Ca}(\text{OH})_2$ as the slurry pH did not decrease at the beginning stage of each carbonation reaction as shown in Fig. 2 and Fig. 3. Thereafter, the slurry pH decreased rapidly in time depending on the CO_2 flow rates. This indicates that the $\text{Ca}(\text{OH})_2$ has been totally carbonated.

The HR area in the Fig. 3 was observed in shorter times within increasing CO_2 flow rate and the use of MBG comparing to the use of OCG. When the reaction was in the HR area, the dissolution rate of CO_2 is larger than its consumption rate

due to absence of Ca^{2+} ion in the solution and the accumulation of H^+ ion leads to the decrease of solution that became acidic [6, 27]. These findings are in line with those of previous studies [23, 25, 28].

Each prepared precipitate was of calcite phase of CaCO_3 with a high purity according to the XRD examination (not given in this paper). The use of MBG did not influence on the morphology of the product. No peaks representing the aragonite or vaterite phase of CaCO_3 were observed. Fig. 4 shows the carbonation time depending on the CO_2 flow rates through the MBG and OCG.

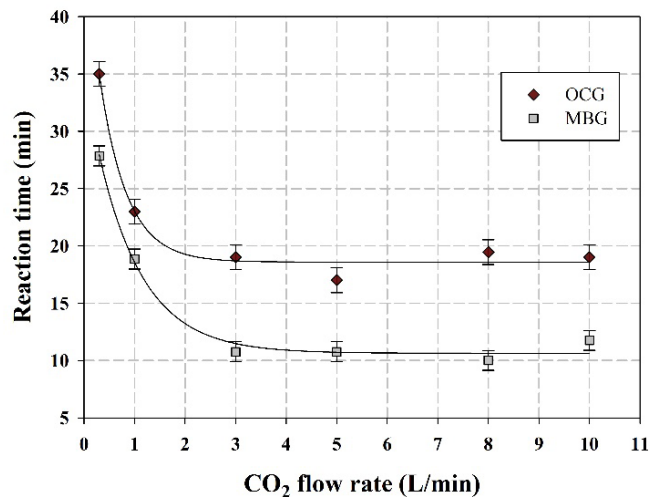


Fig. 4 Change of reaction time depending on CO_2 apparatus

The amount of CO_2 that is necessary for the complete carbonation reaction was the same as the concentration of $\text{Ca}(\text{OH})_2$ was constant for each experiment. At 0.3 L/min of CO_2 flow rate, the longest reaction time was obtained. However, the increase of CO_2 flow rate led to an accelerated carbonation and the growth time of each precipitate decreased. However, the change in the reaction time was minimal at ≥ 3 L/min of CO_2 flow rate, some of CO_2 bubbled into the solution left the carbonation reactor without reacting Ca^{2+} ions. This may be due to the constant absorption ratio of CO_2 at experimental conditions conducted [23, 29, 30].

When the obtained results obtained from both apparatus were compared each other, the MBG has strong effects on the carbonation reaction [19, 25]. The precipitate was obtained in shorter times with the use of MBG compared to the OCG. The surface tension of bubbles increases due to generating tiny bubbles through the MBG that remain longer in the liquid phase and contact with the $\text{Ca}(\text{OH})_2$ in extended times [31, 32]. These properties led to the increase solubility of CO_2 in the slurry, and the reaction became faster [19, 33]. At 0.3 L/min, the reaction time was found to be 35 and 27 min for the MBG and OCG. The percentage of reacted CO_2 was found to be 27% for the MBG and 21% for the OCG at the fixed CO_2 flow rate of 0.3 L/min. respectively (Fig. 5).

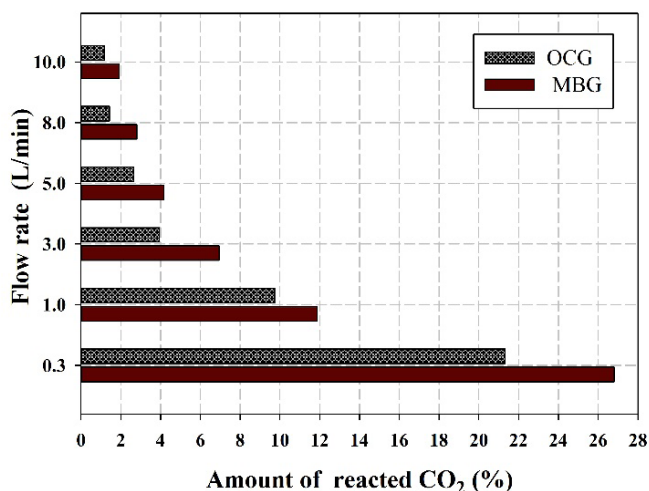


Fig. 5 Amount of reacted CO₂ at various flow rates

However, larger bubbles having low surface tension were produced and escaped easily from the slurry due to buoyancy when the OCG was used [26, 27]. This explains the difference of reaction time between both the MBG and OCG. An increase of up to 5 L/min of CO₂ flow rate lead to the decrease of reaction time. However, there was no change determined in carbonation time at higher CO₂ flow rates. The amount of reacted CO₂ decreased and it left from the reactor without reacting with Ca(OH)₂ and entered the gas holder due to the increase of CO₂ flow rates.

Fig. 6 shows the SEM images of each precipitate obtained through the MBG. It is clear that the morphology and particle size of precipitate was not influenced by the CO₂ flow rates since the MBG generates tiny bubbles at each flow rates. The precipitate was mono-dispersed, uniform and cubic shapes (Fig. 6. (a)-(b)-(c)-(d)-(e)-(f)). The particle size analysis results were consistent with those of findings observed from the SEM examination. The d₉₀ of precipitate was found to be 61.43, 76.45, 86.50, 97.23, 100.42 and 122.40 nm at 0.3, 1, 3, 5, 8 and 10 L/min, respectively. These findings are consistent with those of study [34]. The number of CO₂ bubbles has a no influence on the d₉₀ value as the size of CO₂ bubbles was almost the same size at each CO₂ flow rate. The particle size is relatively uniform and its distribution is narrow. This was due to the dispersion of CO₂ tiny bubbles that led to produce calcite nanoparticles [35].

However, the controlling of CO₂ bubble size through the OCG was impossible at higher CO₂ flow rates. The increase of CO₂ flow rate affected the morphology of precipitate (Fig. 7). This finding was in good agreement with those of previous study [20]. Except for the precipitate prepared at 0.3 L/min (Fig. 7.a), the particles of PCC tend to be agglomerated and poly-dispersed. It was difficult to obtain precipitates of uniform particle size. The smaller crystals appeared on the surface of large crystals of precipitate depending on the CO₂ flow rates as shown in Fig. 7.(b)-(c)-(d)-(e)-(f). Then, the precipitate

with large and small rhombohedral shapes was obtained with increasing CO₂ flow rates. This was confirmed by the d₉₀ of each precipitate prepared using the OCG. The d₉₀ of precipitate was found to be 102.56 nm at 0.3 L/min of CO₂ flow rate, whereas the d₉₀ of precipitate prepared at 10 L/min of CO₂ flow rate was 2.01 μm. It was thought that this was related to the bubble size of CO₂, and bigger CO₂ bubbles led to an obtain PCC in micron sizes in this paper.

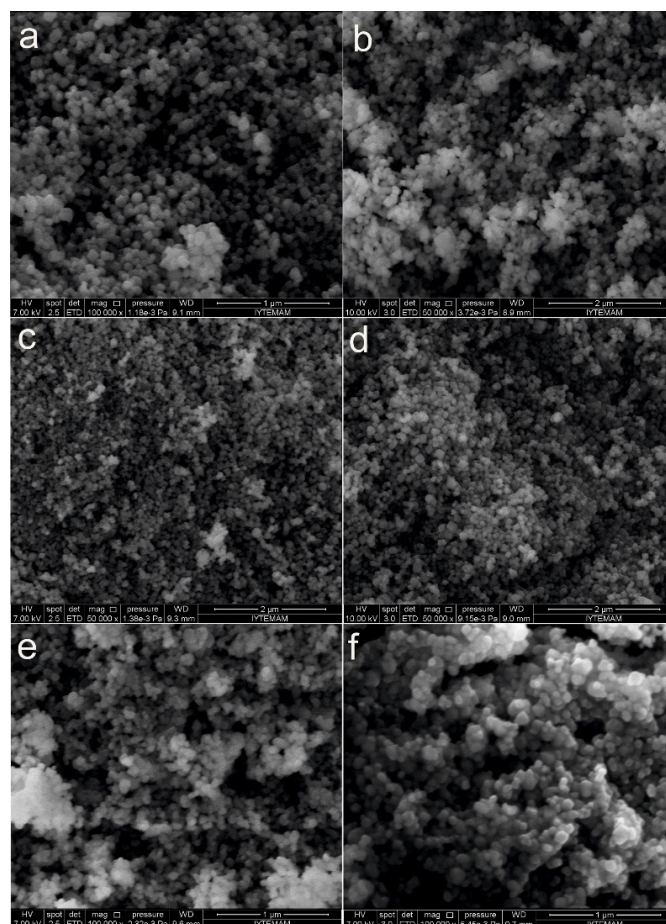


Fig. 6 SEM photograph of precipitates prepared using a MBG: a) 0.3 L/min, b) 1 L/min, c) 3 L/min, d) 5 L/min, e) 8 L/min and f) 10 L/min

Researchers have suggested that the BET surface area is related to the particles diameter (D), or radius (R) and the skeletal density [28, 36]. For that reason, it was assumed that all of the particles were of spherical shapes and non-porous and determined the specific surface area of each product using the following equation. The calculated results are given in Table 1. The precipitates with higher surface areas were obtained by means of the MGB.

$$s_g = \frac{6}{d \cdot p_g} \quad (6)$$

Where, s_g is the specific surface area of precipitate (g/m²), p_g is the density of CaCO₃ (2.711 g/cm³), d is the particle size of precipitate (μm)

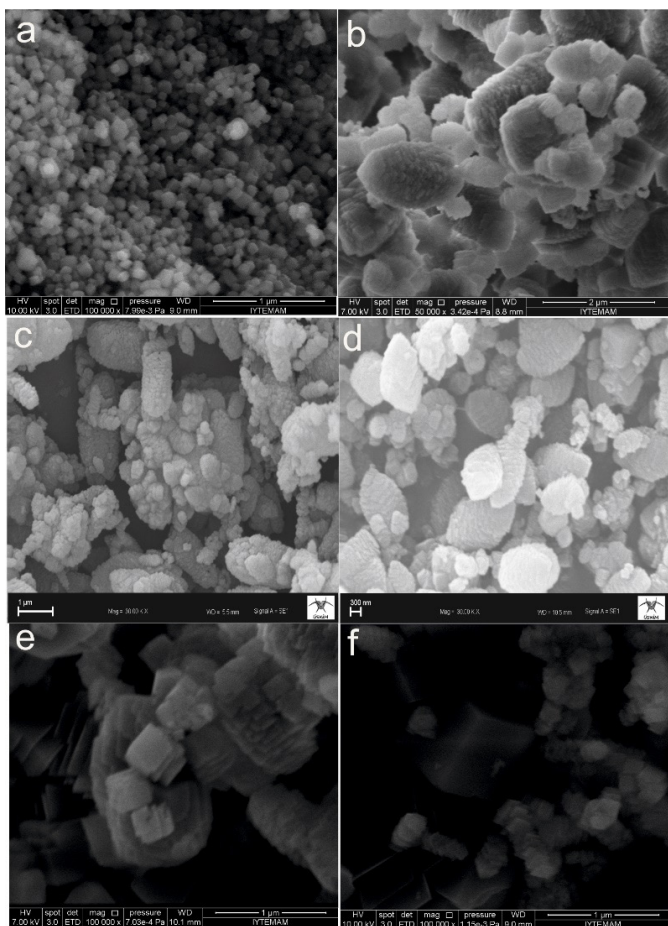


Fig. 7 SEM photograph of precipitates prepared using an OCG: a) 0.3 L/min, b) 1 L/min, c) 3 L/min, d) 5 L/min, e) 8 L/min and f) 10 L/min

Table 1 Particle size and calculated surface area of each precipitate

CO ₂ flow rate (L/min)	Microbubble generator (MGB)		Ordinary CO ₂ generator (OCG)	
	d ₉₀ (nm)	SSA (m ² /g)	d ₉₀	SSA (m ² /g)
0.3	61.43	36.03	102.56 nm	21.58
1	76.45	28.95	1.05 μm	2.11
3	86.5	25.59	1.55 μm	1.43
5	97.23	22.76	1.67 μm	1.33
8	100.42	22.04	1.89 μm	1.17
10	122.4	18.08	2.01 μm	1.11

4 Conclusion

In this paper, the carbonation reaction was facilitated when CO₂ gas was bubbled into the slurry through the MBG. It led to an increase not only the percentage of reacted CO₂ but the carbonation recovery. The SEM images clearly show the influences of both apparatus on the morphology and particle size of precipitates. Calcite nanoparticles were prepared at each CO₂ flow rates by means of the MBG. There was no need to use any chemical to produce calcite nanoparticles (below <125 nm) with the narrow size and uniform morphology. However, an increase in the CO₂ flow rate affected the morphology and

particle size of each precipitate when using the OCG. If the CO₂ flow rate was fast, controlling the diffusion and nucleation of those particles would be difficult, and small&large crystal particles were prepared. The MBG can overcome the difficulty of those problems.

The reaction was complete in shorter times through the MBG that generates tiny bubbles at higher flow rates. This finding was supported with the percentage of reacted CO₂. The MBG apparatus has superior advantages over the OCG due to the decrease of reaction time by 20 – 45 % depending on the flow rates.

Acknowledgement

The project presented in this article is supported by Research Fund Project of Çukurova University [Grant Number: FBA-2017-7912].

References

- [1] Molva, M. "Nano calcite (CaCO₃) production in semi-batch bubble reactor." PhD Thesis, Department of Chemical Engineering, Izmir Institute of Technology, 2011.
- [2] Bang, J. H., Jang, Y. N. "Method of producing carbonate using carbon dioxide microbubbles and carbonate therefor." In: U.S. Patent (Ed.), United States. 2013.
- [3] Tabeii, K., Haruyama, S., Yamaguchi, S., Shirai, H., Takakusagi F. "Study of microbubble generation by a swirl jet." *Journal of Environment and Engineering*. 2(1), pp. 172-182. 2007. <https://doi.org/10.1299/jee.2.172>
- [4] Sebba, F. "Microfoams — An unexploited colloid system." *Journal of Colloid and Interface Science*. 35, pp. 643-646. 1971. [https://doi.org/10.1016/0021-9797\(71\)90223-2](https://doi.org/10.1016/0021-9797(71)90223-2)
- [5] Liu, X., Zhou, J., Zhang, Y., Liu, X., Chen, Y., Yong, X., Wang, S., Zheng, T., Yuan, H. "Continuous process of biogas purification and co-production of nano calcium carbonate in multistage membrane reactors." *Chemical Engineering Journal*. 271, pp. 223-231. 2015. <https://doi.org/10.1016/j.cej.2015.02.086>
- [6] Xiang, L., Xiang, Y., Wen, Y., Wei, F. "Formation of CaCO₃ nanoparticles in the presence of terpineol." *Materials Letters*. 58(6), pp. 959-965. 2004. <https://doi.org/10.1016/j.matlet.2003.07.034>
- [7] Du, L., Wang, Y., Luo, G. "In situ preparation of hydrophobic CaCO₃ nanoparticles in a gas-liquid microdispersion process." *Particuology*. 11(4), pp. 421-427. 2013. <https://doi.org/10.1016/j.partic.2012.07.009>
- [8] Matsumoto, M., Fukunaga, T., Onoe, K. "Polymorph control of calcium carbonate by reactive crystallization using microbubble technique." *Chemical Engineering Research and Design*. 88(12), pp. 1624-1630. 2010. <https://doi.org/10.1016/j.cherd.2010.02.007>
- [9] Matsumoto, M., Isago, M., Onoe, K. "The application of micro - bubbles for dissolution and crystallization of calcium carbonate in gas-liquid-solid system." *Bulletin of the Society of Sea Water Science, Japan*. 58, pp. 475-486. 2004. <https://doi.org/10.11457/swsj1965.58.475>
- [10] Alamdari, A., Alamdari, A., Mowla, D. "Kinetics of calcium carbonate precipitation through CO₂ absorption from flue gas into distiller waste of soda ash plant." *Journal of Industrial and Engineering Chemistry*. 20(5), pp. 3480-3486. 2014. <https://doi.org/10.1016/j.jiec.2013.12.038>

- [11] Chen, P.-C., Tai, C. Y., Lee, K.C. "Morphology and growth rate of calcium carbonate crystals in a gas-liquid-solid reactive crystallizer." *Chemical Engineering Science*. 52(21-22) pp. 4171-4177. 1997. [https://doi.org/10.1016/S0009-2509\(97\)00259-5](https://doi.org/10.1016/S0009-2509(97)00259-5)
- [12] Jung, W.-M., Hoon Kang S., Kim, K.-S., Kim, W.-S., Kyun Choi, C. "Precipitation of calcium carbonate particles by gas-liquid reaction: Morphology and size distribution of particles in Couette-Taylor and stirred tank reactors." *Journal of Crystal Growth*. 312(22), pp. 3331-3339. 2010. <https://doi.org/10.1016/j.jcrysgro.2010.08.026>
- [13] Tamura, K., Tsuge, H. "Characteristics of multistage column crystallizer for gas-liquid reactive crystallization of calcium carbonate." *Chemical Engineering Science*. 61(17), pp. 5818-5826. 2006. <https://doi.org/10.1016/j.ces.2006.05.002>
- [14] Kotaki, Y., Tsuge, H. "Reactive crystallization of calcium carbonate by gas-liquid and liquid-liquid reactions." *The Canadian Journal of Chemical Engineering*. 68(3), pp. 435-442. 1990. <https://doi.org/10.1002/cjce.5450680313>
- [15] Kuusisto, J., Tiittanen, T. Maloney, T. C. "Property optimization of calcium carbonate precipitated in a high shear, circulation reactor." *Powder Technology*. 303, pp. 241-250. 2016. <https://doi.org/10.1016/j.powtec.2016.09.031>
- [16] Ariyaprayoon, J., Leela-Adisorn, U., Supsakulchai, A. "Crystal habit of CaCO₃ under different carbonation methods." *Journal of Metals, Materials and Minerals*. 19(2), pp. 67-72. 2009.
- [17] Sonawane, S. H., Shirsath, S. R., Khanna, P. K., Pawar, S., Mahajan, C. M., Paithankar, V., Shinde, V., Kapadnis, C. V. "An innovative method for effective micro-mixing of CO₂ gas during synthesis of nano-calcite crystal using sonochemical carbonization." *Chemical Engineering Journal*. 143(1-3), pp. 308-313. 2008. <https://doi.org/10.1016/j.cej.2008.05.030>
- [18] Ulkeryildiz, E., Kilic, S., Ozdemir, E. "Rice-like hollow nano-CaCO₃ synthesis." *Journal of Crystal Growth*. 450, pp. 174-180. 2016. <https://doi.org/10.1016/j.jcrysgro.2016.06.032>
- [19] Bang, J.-H., Kim, W., Song, K. S., Jeon, C. W., Chae, S. C., Cho, H.-J., Jang, Y. N., Park, S.-J. "Effect of experimental parameters on the carbonate mineralization with CaSO₄·2H₂O using CO₂ microbubbles." *Chemical Engineering Journal*. 244, pp. 282-287. 2014. <https://doi.org/10.1016/j.cej.2014.01.072>
- [20] Thriveni, T., Ahn, J. W., Ramakrishna, C., Ahn Y. J., Han, C. "Synthesis of nano precipitated calcium carbonate by using a carbonation process through a closed loop reactor." *Journal of the Korean Physical Society*. 68, pp. 131-137. 2016. <https://doi.org/10.3938/jkps.68.131>
- [21] Botha, A., Strydom, C. A. "Preparation of a magnesium hydroxy carbonate from magnesium hydroxide." *Hydrometallurgy*. 62, pp. 175-183. 2001. [https://doi.org/10.1016/S0304-386X\(01\)00197-9](https://doi.org/10.1016/S0304-386X(01)00197-9)
- [22] Juvekar, V. A., Sharma, M. M. "Absorption of CO₂ in a suspension of lime." *Chemical Engineering Science*. 28(3), pp. 825-837. 1973. [https://doi.org/10.1016/0009-2509\(77\)80017-1](https://doi.org/10.1016/0009-2509(77)80017-1)
- [23] Han, Y. S., Hadiko, G., Fuji, M., Takahashi, M. "Effect of flow rate and CO₂ content on the phase and morphology of CaCO₃ prepared by bubbling method." *Journal of Crystal Growth*. 276(3-4), pp. 541-548. 2005. <https://doi.org/10.1016/j.jcrysgro.2004.11.408>
- [24] Skrzypczak, M., Maurer, M. "Process for the production of precipitated calcium carbonate, precipitated calcium carbonate and uses thereof." In: *E.P. Application*. 2011.
- [25] Wei, S.-H., Mahuli, S. K., Agnihotri, R., Fan, L.-S. "High surface area calcium carbonate: pore structural properties and sulfation characteristics." *Industrial & Engineering Chemistry Research*. 36(6), pp. 2141-2148. 1997. <https://doi.org/10.1021/ie9607681>
- [26] Bang, J.-H., Jang, Y. N., Kim, W., Song, K. S., Jeon, C. W., Chae, S. C., Lee, S.-W., Park, S.-J., Lee, M. G. "Precipitation of calcium carbonate by carbon dioxide microbubbles." *Chemical Engineering Journal*. 174(1), pp. 413-420. 2011. <https://doi.org/10.1016/j.cej.2011.09.021>
- [27] Feng, B., Yong, A. K., An, H. "Effect of various factors on the particle size of calcium carbonate formed in a precipitation process." *Materials Science and Engineering: A*. 445-446, pp. 170-179. 2007. <https://doi.org/10.1016/j.msea.2006.09.010>
- [28] Yang, J.-H., Shih, S.-M. "Preparation of high surface area CaCO₃ by bubbling CO₂ in aqueous suspensions of Ca(OH)₂: Effects of (NaPO₃)₆, Na₅P₃O₁₀, and Na₃PO₄ additives." *Powder Technology*. 197(3), pp. 230-234. 2010. <https://doi.org/10.1016/j.powtec.2009.09.020>
- [29] Tokumura, M., Baba, M., Kawase, Y. "Dynamic modeling and simulation of absorption of carbon dioxide into seawater." *Chemical Engineering Science*. 62(24), pp. 7305-7311. 2007. <https://doi.org/10.1016/j.ces.2007.08.074>
- [30] Altiner M., Yildirim, M. "Production and characterization of synthetic aragonite prepared from dolomite by eco-friendly leaching-carbonation process." *Advanced Powder Technology*. 28, pp. 553-564. 2017. <https://doi.org/10.1016/j.apt.2016.10.024>
- [31] Parmar, R., Majumder, S. K. "Microbubble generation and microbubble-aided transport process intensification—A state-of-the-art report." *Chemical Engineering and Processing: Process Intensification*. 64, pp. 79-97. 2013. <https://doi.org/10.1016/j.cep.2012.12.002>
- [32] Xu, Q., Nakajima, M., Ichikawa, S., Nakamura, N., Shiina, T. "A comparative study of microbubble generation by mechanical agitation and sonication." *Innovative Food Science & Emerging Technologies*. 9(4), pp. 489-494. 2008. <https://doi.org/10.1016/j.ifset.2008.03.003>
- [33] Tsuge, H. "Fundamental of microbubbles and nanobubbles." *Bulletin of the Society of Sea Water Science, Japan*. 64, pp. 4-10. 2010. <https://doi.org/10.11457/swsj.64.4>
- [34] Tsutsumi, A., Nieh, J.-Y., Fan, L.-S. "Role of the bubble wake in fine particle production of calcium carbonate in bubble column systems." *Industrial & Engineering Chemistry Research*. 30, pp. 2328-2333. 1991.
- [35] Xiang, L., Xiang, Y., Wang, Z. G., Jin, Y. "Influence of chemical additives on the formation of super-fine calcium carbonate." *Powder Technology*. 126(2), pp. 129-133. 2002.
- [36] Yang, J.-H., Shih, S.-M., Wu, C.-I., Tai, C.Y.-D. "Preparation of high surface area CaCO₃ for SO₂ removal by absorption of CO₂ in aqueous suspensions of Ca(OH)₂." *Powder Technology*. 202(1-3), pp. 101-110. 2010. <https://doi.org/10.1016/j.powtec.2010.04.024>